Characterization of the Unimolecular Water Elimination Reaction from 1-Propanol, 3,3,3-Propan-1-ol-d_3, 3,3,3-Trifluoropropan-1-ol, and 3-Chloropropan-1-ol

Heather A. Ferguson,[†] Caroline L. Parworth,[‡] Traci Berry Holloway,[†] Aaron G. Midgett,[‡] George L. Heard,[‡] D. W. Setser,[§] and Bert E. Holmes*[,‡]

Department of Chemistry, University of North Carolina—Asheville, One University Heights, Asheville, North Carolina 28804-8511, Department of Chemistry, Lyon College, Batesville, Arkansas 72501, and Department of Chemistry, Kansas State University, Manhattan, Kansas 66506

Received: May 28, 2009; Revised Manuscript Received: July 23, 2009

The unimolecular reactions of 1-propanol, 3,3,3-propan-1-ol-d_3, 3,3,3-trifluoropropan-1-ol, and 3-chloropropan-1-ol have been studied by the chemical activation technique. The recombination of CH_3, CD_3, CF_3, and CH_2Cl radicals with CH_2CH_2OH radicals at room temperature was used to generate vibrationally excited $CH_3CH_2CH_2OH$, $CD_3CH_2CH_2OH$, $CF_3CH_2CH_2OH$, and $CH_2ClCH_2CH_2OH$ molecules. The principal unimolecular reaction for propanol and propanol-d_3 with 90 kcal mol^{-1} of vibrational energy is 1,2-H_2O elimination with rate constants of 3.4×10^5 and 1.4×10^5 s^{-1}, respectively. For $CH_2ClCH_2CH_2OH$ also with 90 kcal mol^{-1} of energy, 2,3-HCl elimination with a rate constant of 3.0×10^7 s^{-1} is more important than 1,2-H_2O elimination; the branching fractions are 0.95 and 0.05. For $CF_3CH_2CH_2OH$ with an energy of 102 kcal mol^{-1}, 1,2-H_2O elimination has a rate constant of 7.9×10^5 and 2,3-HF elimination has a rate constant of 2.6×10^5 s^{-1}. Density functional theory was used to obtain models for the molecules and their transition states. The frequencies and moments of inertia from these models were used to calculate RRKM rate constants, which were used to assign threshold energies by comparing calculated and experimental rate constants. This comparison gives the threshold energy for H_2O elimination from 1-propanol as 64 kcal mol^{-1}. The threshold energies for 1,2-H_2O and 2,3-HCl elimination from $CH_2ClCH_2CH_2OH$ were 59 and 54 kcal mol^{-1}, respectively. The threshold energies for H_2O and HF elimination from $CF_3CH_2CH_2OH$ are 62 and 70 kcal mol^{-1}, respectively. The structures of the transition states for elimination of HF, HCl, and H_2O are compared.

1. Introduction

The most important elementary unimolecular reactions of aliphatic alcohols include 1,2-H_2O elimination to give alkenes and the rupture of the weakest C−C or C−OH bonds to give free radicals. The latter lead to free-radical-induced chain reactions under thermal activation conditions, and reliable Arrhenius parameters for the elementary unimolecular steps have been difficult to measure by thermal activation experiments. The elimination of water (or dehydration) as the path with the lowest threshold energy, E_0, for ethanol has only recently been firmly established following infrared multiphoton laser-excitation experiments[1] and observation of infrared emission from H_2O as a product from ethanol molecules formed by recombination of H and CH_2CH_2OH at room temperature.[2] Modern thermal activation studies[3,4] of ethanol with radical inhibitors have succeeded in establishing Arrhenius parameters for the two main elementary reactions. Such work plus extensive modeling and electronic structure calculations[3,5] have reached a consensus value of $E_0 = 66 \pm 2$ kcal mol^{-1} for the dehydration of ethanol. The literature associated with studies of alcohols activated by the insertion of O(^{1}D) atoms into hydrocarbons is very extensive.[6−8] However, the high vibrational energy, ~140 kcal mol^{-1}, of the molecules favors the dissociation channels. The multiple reaction pathways and subsequent free-radical secondary reactions complicate the analysis, and reliable unimolecular rate constants at 140 kcal mol^{-1} for the elementary reactions have been difficult to obtain. Modern studies of O(^{1}D) insertion reactions provide interesting dynamical details about the dissociation processes, but not unimolecular rate constants for the alcohols.[7,8] The difficulty of working with the CH_2OH radical has prevented chemical activation studies of alcohols at more modest energies utilizing recombination of $CH_2OH + R$ (R = CH_3, C_2H_5, etc.), and recombination of OH with R also tend to be chemically complex systems. We have circumvented some of these difficulties by employing the CH_3, CD_3, CF_3, and $CH_2Cl + CH_2CH_2OH$ recombination reactions to generate 1-propanol, 3,3,3-propan-1-ol-d_3, and 3-chloropropan-1-ol molecules with 90 kcal mol^{-1} vibrational energy, as well as 3,3,3-trifluoropropan-1-ol with 102 kcal mol^{-1} of energy. The rate constants for 1,2-H_2O elimination were measured for all molecules, and the rate constants for 2,3-HCl and 2,3-HF elimination also were measured for $CH_2ClCH_2CH_2OH$ and $CF_3CH_2CH_2OH$, respectively. The rate constant for dehydration from $CD_3CH_2CH_2OH$ is simply a statistical secondary kinetic-isotope effect[9,10] that supports the basic model for 1,2-H_2O elimination from propanol. In addition, the $CD_3CH_2CH_2OH$ results will test whether 1,3-DOH elimination occurs as was found for energized propanol ions.[11]

The fundamental goal is to obtain a reliable E_0 value for 1,2-H_2O elimination from 1-propanol. Since the transition state models for HCl elimination have been thoroughly tested,[10,12] the comparison of H_2O and HCl elimination processes from the same molecule should provide some insight for dehydration. As an additional contribution to this effort, the rate constants

* Corresponding author.
[†] Lyon College.
[‡] University of North Carolina—Asheville.
[§] Kansas State University.

10.1021/jp905012r CCC: $40.75
Published on Web 08/24/2009

for HF and H_2O elimination from $CF_3CH_2CH_2OH$ formed with 102 kcal mol^{-1} of energy were measured. If the threshold energy is not affected, the F atoms have the role of a kinetic isotope effect,[9] but the electron-withdrawing CF_3 group usually has an effect on threshold energies.[10,12] For energies of 90−100 kcal mol^{-1}, dissociation reactions of propanol are not competitive with dehydration,[2] which greatly simplifies the chemical reactions in the room temperature system. The loss of H_2O will usually be referred to as dehydration, but H_2O elimination also will be used especially when comparison with the elimination processes of HCl or HF is desired.

The same methodology that we have used for similar experimental studies of halopropanes was employed to assign threshold energies.[10,12−15] Density functional theory (DFT) was used at the B3PW91/6-311+G(2d,p) level to calculate the structures of $CH_3CH_2CH_2OH$, $CD_3CH_2CH_2OH$, $CF_3CH_2CH_2OH$, and $CH_2ClCH_2CH_2OH$ and their transition states. These calculated frequencies and moments of inertia were employed with RRKM theory to calculate the statistical unimolecular rate constants as a function of threshold energy. Comparison of the calculated rate constants to the experimental values permitted assignment of E_0 values. In the RRKM rate constant calculations, torsional motions were treated as hindered internal rotors, which then requires consideration of the conformers for the molecules and transition states.

Dehydration processes can be more easily observed from thermal activation of 2-propanol and 2-methyl-2-propanol than 1-propanol, because the E_0 for dehydration is reduced for secondary and tertiary alcohols, just as is the case for HX (X = F, Cl, Br) elimination reactions.[16−20] Several pyrolysis studies exist for 2-propanol, and a recent theoretical analysis[21] concluded that dehydration is an important channel for most temperatures and pressures. Thermal activation studies of 1-propanol,[19,20] which are not so common, seem to be dominated by free-radical chain reactions. However, Maccoll and Thomas[20] claim to have isolated the dehydration reaction under condition of nitric oxide inhibition and give $A = 4.4 \times 10^{13}$ s^{-1} and $E_a = 66.8$ kcal mol^{-1} as Arrhenius parameters. A recent molecular beam study[22] of $O(^1D)$ + propane did not find evidence for a decomposition channel involving loss of water, perhaps because these products were difficult to observe in the presence of the more important dissociation channels. A recent shock-tube study of the thermal decomposition of CH_2FCH_2OH found that the threshold energy for HF elimination was lower than that for dehydration.[23]

The photolysis of CH_3I, CD_3I, CF_3I, and CH_2ClI with CH_2OHCH_2I at room temperature was used as the source of radicals. Other investigations also have used CH_2OHCH_2I as a satisfactory source of CH_2CH_2OH radicals.[24,25] The expected recombination and disproportionation reactions with these radical are listed below with CH_3 as the example.

$$CH_3 + CH_2CH_2OH \rightarrow CH_3CH_2CH_2OH^* \quad (1)$$
$$\rightarrow CH_4 + CH_2{=}CHOH(\text{or } CH_3CHO)$$

$$2CH_2CH_2OH \rightarrow (CH_2CH_2OH^*)_2 \rightarrow CH_3CH_2OH + CH_2{=}CHOH\ (\text{or } CH_3CHO) \quad (2)$$

$$2CH_3 \rightarrow C_2H_6^* \quad (3)$$

Although vinyl alcohol is stable in the gas phase, it rearranges to acetaldehyde on surfaces and in the column of the gas chromatograph,[26] and acetaldehyde actually is the observed product from the disproportionation reactions. The self-disproportionation-to-recombination ratio for CH_2CH_2OH radicals has been estimated[24] as 0.12. The $C_2H_6^*$ and $(CH_2CH_2OH)_2^*$ molecules will be collisionally stabilized at the pressures of our experiments, which were designed to study the competition between decomposition and collisional stabilization of 1-propanol in bath gas M (CH_3I and CH_2ICH_2OH).

$$CH_3CH_2CH_2OH^* \rightarrow CH_3CH{=}CH_2(D) + H_2O \quad (4)$$

$$+ M \rightarrow CH_3CH_2CH_2OH(S) + M$$

The experimental rate constant for propanol molecules with 90 kcal mol^{-1} of vibrational energy was obtained from the slopes of the usual plots of D/S vs $(\text{pressure})^{-1}$. The chemical equations that describe the $CD_3CH_2CH_2OH$, $CF_3CH_2CH_2OH$, and $CH_2ClCH_2CH_2OH$ systems are analogous to eqs 1−4, although the side reactions for the CH_2Cl and CF_3 systems are somewhat more troublesome and $CH_2ClCH_2CH_2OH^*$ ($CF_3CH_2CH_2OH^*$) can react either by 1,2-H_2O or by 2,3-HCl (2,3-HF elimination) elimination. Although propanal was a persistent product in all three systems, it does not arise from a unimolecular reaction of propanol, rather it is a product from free-radical reactions in the system, vide infra.

II. Experimental Procedures

A. $CH_3CH_2CH_2OH$ and $CD_3CH_2CH_2OH$. Cophotolysis of CH_3I or CD_3I with CH_2ICH_2OH plus small amounts[27] mercury(I) iodide by a high pressure Oriel 6137 200 W high-pressure mercury lamp was used to generate 1-propanol and 1-propanol-*3,3,3-d*$_3$. The iodide samples were measured in a calibrated volume and cryogenically transferred via a grease-free vacuum line to Pyrex glass photolysis vessels varying in volume from 34.7 to 2066 cm^3. A MKS 270 electronic manometer was used for measurement of pressure. The samples consisted of 0.45 μmol of CH_3I and 0.045 μmol of CH_2ICH_2OH, which were irradiated for 5−30 min depending on the size of the vessel. Generally 5−10% of the sample would be converted to products. In Pyrex glass vessels, the effective wavelength range for photolysis is ≥290 nm. The CH_3I, CD_3I, and CH_2ICH_2OH were purchased from Aldrich. Samples were transferred to storage vessels on the vacuum line after several freeze−pump−thaw cycles.

Product identification was based upon data collected with a Shimadzu QP-5000 gas chromatograph with mass spectrometer detector (GC-MS) equipped with a 105 m RTX-624 capillary column. Products were identified by comparison of retention times and mass spectra to commercially available compounds. The temperature program for the separation began with a constant temperature of 35 °C for 20 min followed by increasing the temperature by 6 deg/min until 200 °C was reached. The typical elution times (in minutes) of the major components were $CH_3CH{=}CH_2$ (8), CH_3CH_2CHO (19), CH_3I (20), $CH_3CH_2CH_2OH$ (28), and CH_2ICH_2OH (39). In addition small yields of C_2H_6, C_2H_5OH, and CH_3CHO were observed in accord with reactions 1−3. The acetaldehyde arises from the isomerization of the vinyl alcohol product from reaction 2.[26] The 1,4-butandiol product was not observed, perhaps because it was not eluted from the GC column by the selected temperature program. No evidence was found for propene-d_2 in the $CD_3CH_2CH_2OH$ experiments removing the possibility of a 1,3-HOD elimination pathway that was observed for the propanol cation.[11] In addition

to the expected products, small yields of C_2H_4 were observed. The mechanisms for producing ethene and propanal are considered next.

The mechanism for the generation of CH_3CH_2CHO involves the reaction of vinyl alcohol with CH_3 (CF_3 or CH_2Cl).

$$CH_3 + CH_2{=}CHOH \rightarrow CH_3CH_2CHOH^* \rightarrow CH_3CH_2CHO + H \quad (5)$$

The vibrationally excited $CH_3CH_2CHOH^*$ radical will decompose by loss of an H atom to give the observed CH_3CH_2CHO (or CH_2ClCH_2CHO or CF_3CH_2CHO) product.

The explanation for the presence of C_2H_4 is less certain. Photolysis of CH_2ICH_2OH can generate C_2H_4 at short wavelengths from dissociation of CH_2CH_2OH radicals that have retained enough energy, $\geq$29 kcal mol^{-1}, from the photolysis step or from absorption of a second photon.[28] For 300 nm photolysis, the excess energy is about 40 kcal mol^{-1}. The dissociation of a small fraction of the CH_2CH_2OH radicals that have retained $\geq$29 kcal mol^{-1} of vibrational energy is a possibility, although the photodissociation of ICH_2CH_2OH is expected to favor release of translational energy.[28] A disproportionation reaction involving transfer of OH to CH_3 radicals seems unlikely, since CH_3OH was not observed. Another possibility could be disproportionation between two CH_2CH_2OH radicals giving C_2H_4 and CH_2OHCH_2OH. We are not aware of OH transfer in disproportionation reactions; however, Cl atom transfer in disproportionation has been reported.[10] Other investigators[24] who have used CH_2ICH_2OH as a source of CH_2CH_2OH radicals from photolysis at shorter wavelengths, reported $CH_3CHO + H + I$ as a major competing primary pathway. In our experiments the yield of CH_3CHO was always modest and photolysis at $\geq$290 nm seems mainly to give $CH_2CH_2OH + I$. Our observations are in accord with the study at 266 nm.[28a]

The ratios of $CH_3CH{=}CH_2/CH_3CH_2CH_2OH$ and $CD_3CH{=}CH_2/CD_3CH_2CH_2OH$ were measured at various pressures using a Shimadzu GC-14A gas chromatograph with a flame-ionization detector (GC-FID) and the 105 m MXT-624 column. Whenever possible the FID detector is preferred to MS because calibration factors are more accurate and because larger samples can be analyzed. The temperature program was the same as mentioned for the experiments using the GC-MS analysis. Since commercial samples were available, the response of the GC-FID could be calibrated, and the calibration factor for the ratio of peak areas of propene to propanol was 1.7. The greatest difficulty in obtaining reliable data was quantitative gas handling of the propanol and CH_2ICH_2OH because of their tendency to adsorb on Pyrex glass walls. Thus, care and patience was necessary to ensure complete transfer of a gas samples under cryogenic pumping.

B. $CH_2ClCH_2CH_2OH$. Chemically activated $CH_2ClCH_2CH_2OH$ molecules were prepared by photolysis of mixtures typically containing 0.11 μmol of CH_2ClI (purchased from Aldrich) and 0.33 μmol of ICH_2CH_2OH and 8.8 μmol of SF_6 in Pyrex vessels containing small amounts of mercury(I) iodide. The photolysis experiments were done at room temperature in vessels ranging in volume from 67 to 852 cm^3. The vessels were irradiated for 2−5 min depending on the vessel size, and typically 50% of the iodide precursors were consumed.

Products were identified with a Shimadzu QP5000 GC-MS equipped with a 105 m Rtx-200 column. A Shimadzu GC-14A gas chromatograph with flame ionization detection operated with a 105 m RTX-200 column of 0.53 mm i.d. was used to measure the ratios of decomposition to stabilization (D_i/S) at various pressures. Similar temperature programs were used for the GC-MS and GC-FID^{-1} analyses; the oven was set at 35 °C for 10 min, then the temperature was increased to 200 °C at a heating rate of 2 °C min^{-1}. The following products and reactants (with typical retention times in min.) were identified: $CH_2{=}CH_2$ (10), $CH_2{=}CHCl$ (12), $CH_2{=}CHCH_2Cl$ (20), $CH_2{=}CHCH_2OH$ (23), CH_2ClCH_2CHO (25), CH_2ClCH_2Cl (31), CH_2ClI (39), $CH_2ClCH_2CH_2OH$ (58), and CH_2OHCH_2I (60). The $CH_2{=}CHCl$ arises from HCl loss from chemically activated 1,2-dichloroethane. Commercial samples of all important products were available to provide positive identification.

Since the primary data for the D_i/S ratios were obtained with the GC-FID system, a calibration of the relative response was necessary. The ratio of response factors for $CH_2{=}CHCH_2OH$, $CH_2{=}CHCH_2Cl$, and $CH_2ClCH_2CH_2OH$ were determined from mixtures with a composition that mimics the photolyzed samples. The response factors were 1.41 ± 0.37 for $CH_2{=}CHCH_2OH/CH_2ClCH_2CH_2OH$ and 1.93 ± 0.26 for $CH_2{=}CHCH_2Cl/CH_2ClCH_2CH_2OH$.

C. $CF_3CH_2CH_2OH$. Using the same procedures as described for $CH_3CH_2CH_2OH$, a series of experiments were done with photolysis of 2.68 μmol of ICH_2CH_2OH and 0.889 μmol of CF_3I to create vibrationally excited $CF_3CH_2CH_2OH$ molecules. The CF_3I was purchased from SynQuest.

A Hewlett-Packard 5890/579 GC-MS fitted with a 105 m × 0.25 mm Restek RTX-200 capillary column was used for identification of the products and measurement of the alkene/alcohol ratio. Using an initial temperature of 35 °C for 15 min followed by temperature programming at 10 °C per min to a final temperature of 150 °C, the normal elution times (in min.) were generally as follows: CF_3CF_3 (10), $CF_3CH{=}CH_2$ (11), CF_3I (12), $CF_3CH_2CH_2CF_3$ (13), CH_3CH_2OH (15), CH_3CHO (16), CF_3CH_2CHO (19), $CF_2{=}CHCH_2OH$ (22), $CF_3CH_2CH_2OH$ (23), and ICH_2CH_2OH (37). A commercial sample of $CF_2{=}CHCH_2OH$ was not available, but the GC peak assigned to this molecule had the expected pressure dependence relative to $CF_3CH_2CH_2OH$, and the mass spectrum (relative abundances) was $CF_2{=}CHCH_2O^+$(100), CF_2H^+ (92), $CFCHCH_2O^+$ (92), $CFCHCHO^+$ (89), and $CFCH_2^+$ (80). The response of the GC-MS total ion count for $CF_3CH_2CH_2OH$ and for $CF_3CH{=}CH_2$ was determined using five trials of three independently prepared samples designed to replicate the photolysis samples. The calibration factor for the $[CF_3CH{=}CH_2]/[CF_3CH_2CH_2OH]$ ratio was 0.99. Since a commercial sample of $CF_2{=}CHCH_2OH$ was not available, it was assumed that the response of the mass spectrometer would be similar to that of $CH_2{=}CHCH_2OH$. The calibration factor for the $[CH_2{=}CHCH_2OH]/[CF_3CH_2CH_2OH]$ ratio was measured as 1.4. The $CF_3CH{=}CH_2$ from reaction 6c was subtracted from the total $CF_3CH{=}CH_2$ yield to obtain the component from the decomposition of $CF_3CH_2CH_2OH$. The yield from (6c) was

$$CF_3 + C_2H_4 \rightarrow CF_3CH_2CH_2 \quad (6a)$$

$$CF_3 + CF_3CH_2CH_2 \rightarrow CF_3CH_2CH_2CF_3 \quad (6b)$$

$$\rightarrow CF_3H + CF_3CH{=}CH_2 \quad (6c)$$

deduced from the quantity of $CF_3CH_2CH_2CF_3$ and the published[29] disproportionation to combination ratio (0.022) of the $CF_3CH_2CH_2$ and CF_3 radicals. The fraction of the total

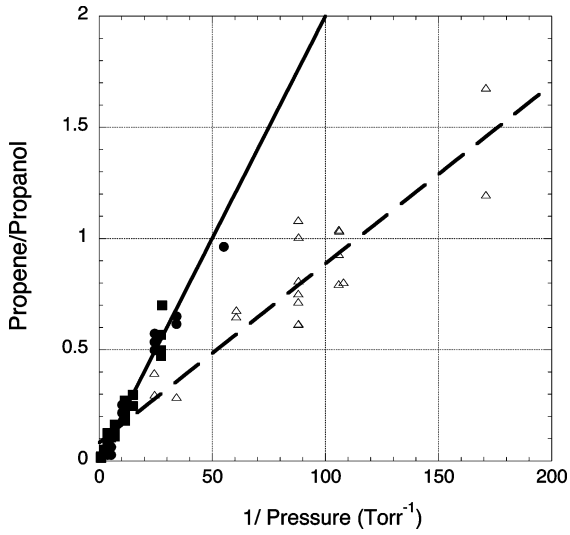

Figure 1. Plot of propene/propanol (D/S) vs (pressure)$^{-1}$ for $CH_3CH_2CH_2OH$ (●, ■) and $CD_3CH_2CH_2OH$* (△). The ● and ■ symbols denote two independent series of experiments, which were combined to obtain a line with a slope of 0.019 ± 0.001 Torr, an intercept of 0.01 ± 0.02, and a correlation coefficient of 0.97. The slope and intercept from the $CD_3CH_2CH_2OH$ data are 0.0081 ± 0.0005 Torr and 0.08 ± 0.04 with a correlation coefficient of 0.95.

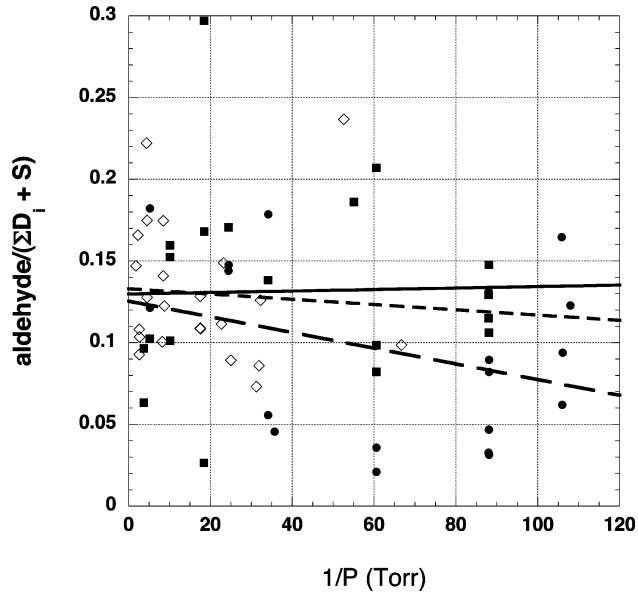

Figure 2. Plot of propanal/(propanol + propene) vs (pressure)$^{-1}$ for $CH_3CH_2CH_2OH$ (■ with a solid line) and $CD_3CH_2CH_2OH$(● with a dash-dot line). Plot of $CF_3CH_2CHO/(CF_3CH_2CH_2OH + CF_3CH{=}CH_2 + CF_2{=}CHCH_2OH)$ vs (pressure)$^{-1}$ (◇ with a dashed line). The nearly constant ratio suggests that the aldehyde is formed in a parallel process to reaction 1 for all of the chemically activated alcohols.

$CF_3CH{=}CH_2$ from (6c) ranged from 0.00 to 0.06, and this correction had an insignificant effect on the ratio of $CF_2{=}CH$-$CH_2OH/CF_3CH_2CH_2OH$.

III. Experimental Results

A. Rate Constants. Rate constants were obtained from linear fits to plots of propene/1-propanol (or D/S) vs (pressure)$^{-1}$ for pressure ranges such that D/S was ≤1.0 for 1-propanol and ≤1.6 for 1-propanol-d_3. Two independent sets of data, separated in time by 3 years, for 1-propanol are shown in Figure 1. The two sets of data are in excellent agreement, and they were combined to obtain the rate constant of k_{expt} = 0.019 ± 0.001 Torr for dehydration of 1-propanol. The rate constant for dehydration is 60 times smaller than the HF elimination rate constant for 1-fluoropropane,[10a] which implies that E_0 is higher for dehydration. The data for 1-propanol-d_3 were collected at the same time as the last set of experiments for 1-propanol. The data points for propanol-d_3 are somewhat more scattered than those for $CH_3CH_2CH_2OH$; however, k_{expt} = 0.0081 ± 0.0005 Torr is in the range expected for a secondary kinetic-isotope effect, k_H/k_D = 2.3, which involves three deuterium atoms.

As previously mentioned, CH_3CH_2CHO (or CD_3CH_2CHO) was observed as a product in the system. A plot of the $CH_3CH_2CHO/CH_3CH_2CH_2OH$ ratio was not consistent with a normal D/S plot; the points are quite scattered and the high-pressure intercept is not zero. Although the data points in a plot of $CH_3CH_2CHO/(CH_3CH_2CH_2OH + CH_2{=}CHCH_3)$ vs (pressure)$^{-1}$, see Figure 2, are scattered, the ratio is nearly constant, which implies a parallel mechanism for the formation of propanal. We believe that it is formed from the reaction of CH_3 (or CD_3) with $CH_2{=}CHOH$, e.g., reaction 5. Similar plots of aldehyde/(S + ΣD$_i$) vs inverse pressure for $CF_3CH_2CH_2OH$ and $CD_3CH_2CH_2OH$ were also nearly constant, see Figure 2, and the results are consistent with formation of the aldehyde from the reaction of CF_3 or CD_3 with $CH_2{=}CHOH$, respectively.

The D_i/S plots for $CF_3CH_2CH_2OH$ are shown in Figure 3; the rate constants are 0.046 ± 0.003 and 0.015 ± 0.001 Torr for elimination of H_2O and HF, respectively. On the basis of

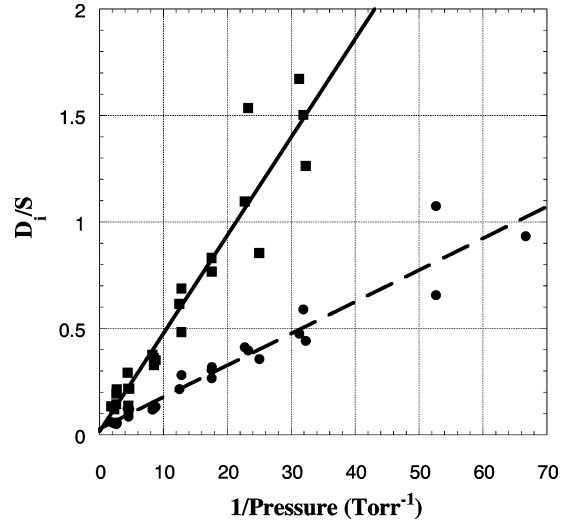

Figure 3. Plot of D_i/S vs (pressure)$^{-1}$ for $CF_3CH_2CH_2OH$: ■, $CF_3CH{=}CH_2/CF_3CH_2CH_2OH$ with slope = 0.046 ± 0.004 Torr and intercept = 0.017 ± 0.047 with correlation coefficient = 0.96; ●, $CF_2{=}CHCH_2OH/CF_3CH_2CH_2OH$ with slope = 0.015 ± 0.001 Torr and intercept = 0.030 ± 0.020 with correlation coefficient = 0.97.

these 25 experiments, the branching ratio for $CF_3CH{=}CH_2/CF_2{=}CHCH_2OH$ is 3.0 ± 0.2. These data seem reliable, and the principal uncertainty in the rate constants probably is the calibration factors of the GC analysis.

The rate constants for $CH_2ClCH_2CH_2OH$ were obtained from the data shown in Figure 4, which are in the pressure range corresponding to D/S ≤ 2. Elimination of HCl is 20 times more important than elimination of H_2O. The rate constants obtained from linear fits to the D/S plots are 1.89 ± 0.07 and 0.093 ± 0.009 Torr for elimination of HCl and H_2O, respectively. Both D/S plots in Figure 4 have intercepts of zero. These data for $CH_2{=}CHCH_2OH$ formation seem to be very reliable. However, the small branching ratio, 0.05, for $CH_2ClCH{=}CH_2$ formation makes $k(H_2O)$ less reliable and the actual uncertainty probably

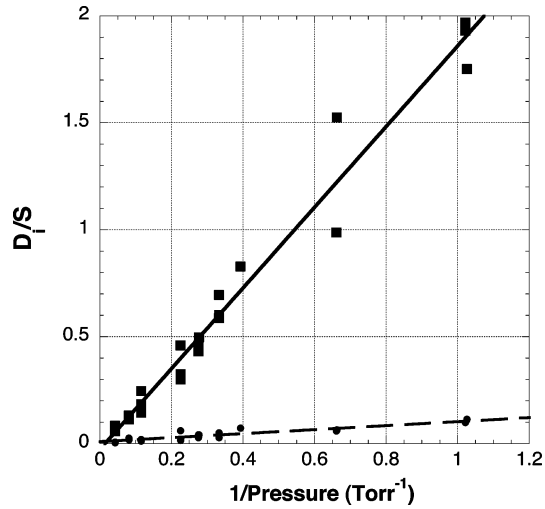

Figure 4. Plot of D_i/S vs $(\text{pressure})^{-1}$ for $CH_2ClCH_2CH_2OH$: ■, $CH_2{=}CHCH_2OH/CH_2ClCH_2CH_2OH$ with slope = 1.89 ± 0.07 Torr and intercept = −0.03 ± 0.03 with correlation coefficient of 098; ●, $CH_2ClCH{=}CH_2/CH_2ClCH_2CH_2OH$ with slope = 0.093 ± 0.009 Torr and intercept of 0.01 ± 0.004 with correlation coefficient = 0.87.

TABLE 1: Experimental Rate Constants

molecule		rate constants[a] Torr	rate constants[a] (10^5) s^{-1}
$CH_3CH_2CH_2OH$	$(-H_2O)^b$	0.019 ± 0.001	3.4 ± 0.6
$CD_3CH_2CH_2OH$	$(-H_2O)^b$	0.0081 ± 0.0005	1.4 ± 0.3
$CF_3CH_2CH_2OH$	$(-H_2O)^c$	0.046 ± 0.004	7.9 ± 1.5
	$(-HF)^c$	0.015 ± 0.001	2.6 ± 0.5
$CH_2ClCH_2CH_2OH$	$(-HCl)^d$	1.89 ± 0.07	297 ± 60
	$(-H_2O)^d$	0.093 ± 0.009	15 ± 3

[a] The rate constants in s^{-1} units were obtained from $k_{expt} = N\pi d^2(8kT/\pi\mu)^{1/2}\Omega^{2,2*}$ with N being the concentration for the cited rate constant in Torr units and for the following collision diameters and ε/k values:[30,31] CH_3I (4.6 Å, 405 K); CF_3I (5.1 Å, 288 K); CH_2ICH_2OH (5.3 Å, 465 K); $CH_3CH_2CH_2OH$ (4.87 Å, 480 K); $CF_3CH_2CH_2OH$ (5.37 Å, 450 K); $CH_2ClCH_2CH_2OH$ (5.5 Å, 500 K); SF_6(5.20 Å, 212 K). [b] The bath gas was CH_3I (CD_3I) + CH_2ICH_2OH in a 10:1 ratio in favor of CH_3I. [c] The bath gas was CF_3I + CH_2ICH_2OH in a 1:3 ratio in favor of CH_2ICH_2OH. [d] The bath gas was CH_2ICl + CH_2ICH_2OH + SF_6 in a 1:3:80 ratio, respectively.

is ±30% rather than ±10%. The dehydration rate constant for $CH_2ClCH_2CH_2OH$ is four to five times larger than the rate constant for 1-propanol, which requires a lower $E_0(H_2O)$ for chloropropanol.

All six rate constants are summarized in Table 1 together with their corresponding values in s^{-1}. The latter were obtained from the collision parameters[30,31] described in the footnote of the table. Since some uncertainty exists for the collision cross sections, the overall uncertainty of the experimental rate constants in s^{-1} units was increased to ±20%.

B. Thermochemistry. The average vibrational energy of the three activated molecules is needed in order to compare calculated rate constants, k_E with $k_{\langle E\rangle}$(expt) values. Since the activation energies for radical recombination reactions are zero, or nearly zero, the average energy for 1-propanol can be obtained from eq 7.

$$\langle E\rangle = D_0(CH_3{-}CH_2CH_2OH) + 3RT + \langle E_{vib}(CH_3)\rangle + \langle E_{vib}(CH_2CH_2OH)\rangle \quad (7)$$

The bond dissociation energy of propanol, which is the critical quantity, can be obtained from experimentally determined enthalpies of formation at 298 K. The values are 35.0, −7.4, and 61.0, kcal mol^{-1} for CH_3,[32] CH_2CH_2OH,[33,34] and 1-C_3H_7OH,[34] respectively, which lead to $D_{298}(CH_3{-}CH_2CH_2OH)$ = 88.6 kcal mol^{-1}. The uncertainty, which should be ≤2 kcal mol^{-1}, mainly depends on $\Delta H°_f(CH_2CH_2OH)$. Converting to 0 K gives $D_0(CH_3{-}CH_2CH_2OH)$ = 87.4 kcal mol^{-1}. Adding the average vibrational energies of the radicals gives $\langle E(\text{propanol})\rangle$ = 90.1 kcal mol^{-1}. The average energy of 1-propanol-d_3 only increases by 0.2 kcal mol^{-1}.

As far as we know, a value for $\Delta H°_f(CF_3CH_2CH_2OH)$ has not been reported. However, a reasonable estimate for $D(CF_3{-}CH_2CH_2OH)$ can be obtained from $D(CF_3{-}CH_2CH_3)$. Using −112.0, 28.9, and −185.3 kcal mol^{-1} for enthalpies of formation of CF_3,[35] C_2H_5,[32] and $CF_3CH_2CH_3$,[36] respectively, gives $D_{298}(CF_3{-}CH_2CH_3)$ = 101.2 kcal mol^{-1}, which we will use for $D_{298}(CF_3{-}CH_2CH_2OH)$. Thus, $\langle E(CF_3CH_2CH_2OH)\rangle$ is ≅12 kcal mol^{-1} higher than $\langle E(CH_3CH_2CH_2OH)\rangle$ or 102 kcal mol^{-1}.

Since $D_{298}(CH_3{-}CH_2CH_2OH)$ is nearly the same as $D_{298}(CH_3{-}CH_2CH_3)$, we expect that $D_{298}(CH_2Cl{-}CH_2CH_2OH)$ will be similar to $D_{298}(CH_2Cl{-}CH_2CH_3)$. On the basis of $D_{298}(CH_2Cl{-}CH_2CH_3)$[34] = 88.2 ± 2.0 kcal mol^{-1}, we assigned $\langle E(CH_2ClCH_2CH_2OH)\rangle$ as 90 ± 2 kcal mol^{-1}.

IV. Assignment of Threshold Energies

A. Models for Molecules and Transition States. Threshold energies, E_0, were assigned by matching experimental rate constants at energy $\langle E\rangle$ to calculated statistical rate constants, k_E, with E_0 as a variable.

$$k_E = s^\dagger/h(I^\dagger/I)^{1/2}\Sigma P^\dagger(E - E_0)/N^*(E) \quad (8)$$

The sums of internal states, $\Sigma P^\dagger(E - E_0)$, of the transition state, and of the density of states, $N^*(E)$, of the molecule were evaluated from models obtained from electronic structure calculations. The $I^\dagger/I$ term is the ratio of the product of the three overall moments of inertia and $s^\dagger$ is the reaction path degeneracy. Calculations for k_E were done with the Multiwell code.[37] A summary of the models for the molecules and transition states is provided in the Supporting Information. The measured rate constants correspond to high-pressure limiting values, which will be assumed to be equivalent to the unit deactivation rate constants. This assumption will be examined more carefully for SF_6 as the bath gas in the Discussion.

The electronic structure calculations were done with the Gaussian code[38] using density functional theory, DFT, at the B3PW9/6-311+G(2d,p) level. In addition several calculations were done with the 6-31G(d′,p′) basis set. The torsional modes of the molecule and transition state were treated as symmetric, hindered, internal rotations in the calculation of $\Sigma P^\dagger(E - E_0)$ and $N^*(E)$. Li, Kazakov and Dryer[3] have noted the importance of the loss of the OH and CH_3 internal rotations in the transition state for calculation of the dehydration rate constant for ethanol, and similar considerations apply to propanol.

The five distinct conformers (four have mirror images) of propanol have been investigated by several authors,[39−41] and the differences in reported energies of the conformers are less than 1 kcal mol^{-1}. Our calculations with the 6-311+G(2d,p) basis set gave similar results with the largest energy difference between conformers of only 0.2 kcal mol^{-1}. The calculated harmonic frequencies and overall moments of inertia, which

are provided in tables in Supporting Information, are in accord with previous calculations and experimental results. We used the geometric average of the conformer frequencies, although they are actually nearly identical, in the calculation of N*(*E*). The barrier to internal rotation of the OH group (I_{red} = 0.78 amu Å^2) is only 1.1 kcal mol^{-1}, and it is nearly a free rotor. The barriers for CH_3 and CH_2OH rotation (I_{red} = 2.86 and 9.52 amu Å^2) are 3.0 and 3.8 kcal mol^{-1}, respectively.[39]

The transition state for dehydration from ethanol resembles the four-membered transition state for HF elimination from fluoroethane.[2,3,23] The *R*(C−H) bond is extended by 30%, the *R*(C−O) bond is extended by 28% and the C−C bond is between a single and double bond. The *R*(H−OH) bond is 30% longer than the bond of water. The four-membered ring is just slightly nonplanar with the OH bond extending away from the plane at an angle of about 110°. The carbon atoms in the ring have considerable sp^2 character; however, the carbon atom attached to the O, F, or Cl atoms develops more sp^2 character in this series, as the diagrams in Figure 5 illustrate. The basic nature of the transition state for dehydration of propanol is the same as just described for ethanol with the additional complication that the OH group can have cis and trans geometries with respect to the CH_3 group; see Figure 5 and Table S-1 in Supporting Information. Each of these cis or trans geometries also has a mirror image as seen in Table S-1 in Supporting Information and illustrates the reactions path degeneracy of four. It appears that the cis or trans isomers form when the proton that is eliminated forms an O−H bond with either of the two lone electron pairs on the oxygen. Since the energy difference between the two isomers is very small, we evaluated the sums of states for the transition state with the average frequencies of the two isomers. The $I^{\dagger}_{red}(CH_3)$ was 2.92 amu Å^2, and the barrier was assumed to be the same as for propanol. The calculated threshold energy for dehydration was 63 and 65 kcal mol^{-1} from the 6-311+G(2d, p) and 6-31G(d′,p′) basis sets, respectively. The calculated threshold energy for H_2 elimination to give propanal was 18 kcal mol^{-1} higher than that for dehydration.

The same set of calculations was done for $CD_3CH_2CH_2OH$ with appropriate reduced moments of inertia for the internal rotations. The barriers for the three hindered rotors were taken to be the same as for propanol. The calculated threshold energy was unchanged from propanol, as expected for a pure secondary kinetic-isotope effect.

The $CF_3CH_2CH_2OH$ system has the same basic structure as propanol, but with the addition of the 2,3-HF elimination pathway in competition with dehydration. The conformers of $CF_3CH_2CH_2OH$ have one complication. Although the energy differences are relatively small, the conformers fall into two categories based upon the lowest frequency, the CF_3 torsion, or upon $I_{red}(CF_3)$. If the OH group is oriented toward the CF_3 group (three conformers) the frequency is lower (I_{red} is larger), whereas if the OH group is oriented away from the CF_3 group (two conformers) the frequency is higher (I_{red} is lower). For the torsional model, the density of states at 100 kcal mol^{-1} was 25% higher for the conformers with the higher CF_3 torsional frequency, because overall the frequencies are lower, even though the CF_3 frequency is higher. Replacing the three torsion frequencies by internal rotors reversed the situation, and the density of states is 20% higher for the conformers with the larger $I_{red}(CF_3)$. Although 20% is still significant, adoption of the hindered-rotor model reduces the difference in the rate constants between the two sets of conformers because the moments of inertia for overall rotation are larger for the category with small I_{red} and the difference in rate constants is actually only 5%. We did rate constant calculations for both categories and averaged the values to compare to experimental rate constants. The H_2O transition state has cis and trans isomers, but only one conformer associated with the CF_3 hindered internal rotation. The HF transition state has the OH and CH_2OH hindered internal rotors, which provide several conformers; the frequencies and moments of inertia of the lowest energy conformer were used for rate constant calculations. The potential barriers were 4.5, 3.8, and 1.0 kcal mol^{-1} for the CF_3, CH_2OH, and OH internal rotors, respectively. Threshold energies were calculated based on the lowest energy conformers; the values were 63.4 and 60.4 kcal mol^{-1} for HF and H_2O elimination, respectively, from the 6-311+G(2d,p) basis set and 68.3 and 61.9 kcal mol^{-1} from the 6-31G(d′,p′) basis set. The E_0(HF) values involving a CF_3 group are usually in the 68−70 kcal mol^{-1} range and the 6-31G(d′,p′) results usually are closer to the experimental values.[10−14] Exchanging a CH_3 for a CF_3 group seems to slightly (2−3 kcal mol^{-1}) decrease the threshold energy for dehydration. The structures of the dehydration transition states for propanol and trifluoropropanol can be compared in Figure 5 and in the Tables S-1 and S-2 in Supporting Information. There are substantial differences; the OH bond is more nearly formed for $CF_3CH_2CH_2OH$, i.e., the R(C−H) and R(C−C) are longer and the R(O−H) and R(C−O) are shorter for $CF_3CH_2CH_2OH$.

The $CH_2ClCH_2CH_2OH$ molecule has an asymmetric CH_2Cl internal rotor, which introduces the complexity associated with 27 conformers. These conformers have been investigated by Yamanaka et al.[42] We decided to select the 5 lowest energy structures to represent the molecule, which actually includes 10 conformers. The average frequencies of these 10 conformers together with the moments of inertia and the reduced moments for the hindered internal rotations, see Table S-3 in Supporting Information, were used for eq 8. The lowest energy conformer for each transition state was used to evaluate $\Sigma P^{\dagger}(E - E_0)$. The barriers to internal rotation for OH and CH_2OH were assumed to be the same as those for propanol. The potential for the CH_2Cl torsion probably depends on the orientation of the OH group;[42] i.e., it will change with conformer. We did calculations with barriers of 4 and 6 kcal mol^{-1} for the CH_2Cl rotor to evaluate the sensitivity to this aspect of the model; the difference in N_E* was 14%. The very large number of conformers for the $CH_2ClCH_2CH_2OH$ system reduces the assignment of a single E_0 to an approximation of reality. The calculated, 6-311+G(2d,p) basis set, threshold energies based on lowest energy conformers were 60.5(trans) and 63.3(cis) kcal mol^{-1} for H_2O elimination and 51.2 kcal mol^{-1} for HCl elimination. The structure of the transition state for dehydration from $CH_2ClCH_2CH_2OH$ resembles that for $CF_3CH_2CH_2OH$ as shown in Figure 5 and Tables S-2 and S-3 in Supporting Information.

B. The Threshold Energies. Since hindered-rotor models are the most realistic representation for these unimolecular reactions, those calculated k_E were used to assign E_0 values, although calculations were done with free-rotor and vibrational models for comparison. The rate constants for the free-rotor model were nearly the same as those for the hindered-rotor case, which implies that the rate constants at 90−100 kcal mol^{-1} are not sensitive to modest changes in barrier heights (as was found explicitly for $CH_2ClCH_2CH_2OH$). However, the rate constants for the hindered-rotor models were substantially smaller, a factor of 8 for propanol, than the rate constants for the vibrational models. For all three molecules the reaction path degeneracy for elimination of H_2O was set as 4, because of the two isomeric transition states. The measured rate constants correspond to high pressure limiting values. These will be assumed to be equivalent

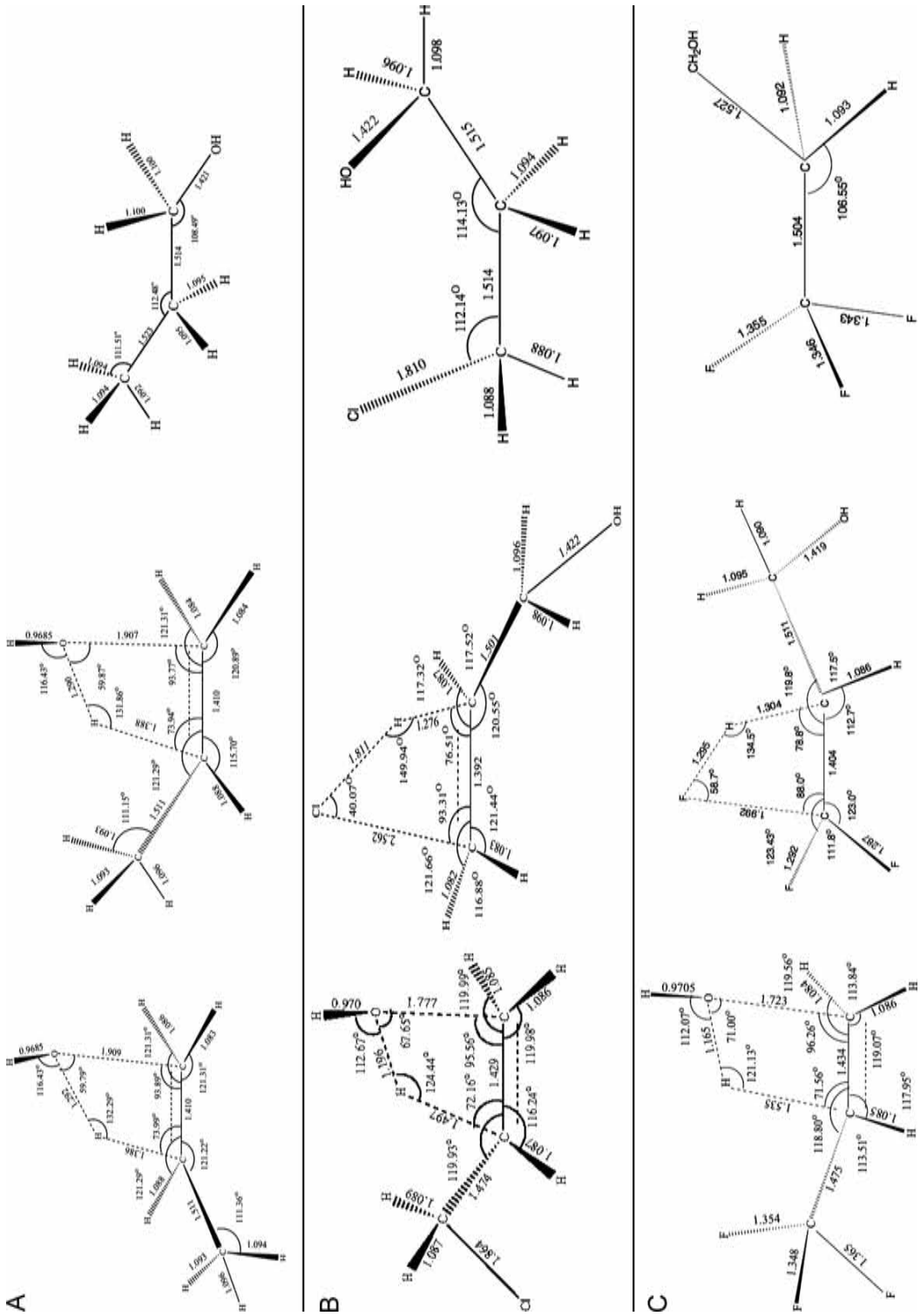

Figure 5. Diagrams of the transition states showing the calculated distances between the atoms in the four-membered rings for the HF, HCl, and H_2O transition states. (A) The two isomeric transition states for HOH elimination and for propanol are shown. The degree of sp^2 character of the carbons involved in the four-member ring in the transition state can be judged by considering how far the tetrahedral geometry of the reactant has progressed to a linear geometry in the transition state. The angle between the triangular plane defined by the CH_2 and an imaginary line extending along the C═C is 24° and the corresponding angle between the triangular plane defined by the CH_3-C-H and the line along the C═C is 26°. Henceforth we will refer to this angle as the hybridization index angle (HIA). For reference an sp^3 carbon will have a HIA of 55° and, of course, an sp^2 carbon will have a HIA of zero. Table S-1 in Supporting Information shows a ball and stick model of the molecule and the two transition state isomers and their enantiomers from the Gaussian output. (B) Transition states for HCl and HOH elimination and the $CH_2ClCH_2CH_2OH$ molecule are shown. Since the transition states for dehydration are all similar, the cis and trans isomers are not shown. For the HOH elimination transition state the HIA is 24° at the CH_2 and 32° at the $CH_2Cl-C-H$, respectively. For the HCl loss transition state the HIA is just 2° on the carbon losing the Cl and 21° at the other carbon. Thus, the carbon with the departing Cl is essentially sp^2 hybridized in the transition state. Table S-3 in Supporting Information shows the ball and stick models. (C) Transition states for HF and HOH elimination and the $CF_3CH_2CH_2OH$ molecule are shown. The isomeric HOH elimination transition states are not shown. Table S-2 in Supporting Information has ball and stick models. For the transition state for HOH loss, the HIA is 26° at the carbon losing the oxygen and is 26° at the middle carbon. The transition state for HF loss has a HIA = 13° at the carbon losing the F equal and HIA is 31° at the carbon losing the hydrogen.

TABLE 2: Comparison of Calculated and Experimental Rate Constants

molecule	$\langle E \rangle$ (kcal mol^{-1})	rate constants (s^{-1}) k_{exp}	$k_{\langle E \rangle}$	E_0 (kcal mol^{-1})
$CH_3CH_2CH_2OH(-H_2O)$	90.0[a]	3.4×10^5	3.3×10^5	64[b]
$CD_3CH_2CH_2OH(-H_2O)$	90.2[a]	1.4×10^5	1.6×10^5	64
$CF_3CH_2CH_2OH(-H_2O)$	102	7.9×10^5	8.0×10^5	62
$(-HF)$	102	2.6×10^5	2.7×10^5	70
$CH_2ClCH_2CH_2OH(-HCl)$	90	3.0×10^7	2.7×10^7	54
		(2.0×10^7)	(1.8×10^7)	(55[c])
$(-H_2O)$	90	1.5×10^6	8.6×10^5	59
		(1.0×10^6) (0.57×10^5)	(0.57×10^5)	(60[c])
$CH_3CH_2CH_2F(-HF)$[d]	94	17×10^6	20×10^6	59
$CH_3CH_2CH_2Cl(-HCl)$[d]	90	87×10^6	104×10^6	54
$CF_3CH_2CH_2Cl(-HCl)$[d]	94	2.4×10^6	2.8×10^6	58
$(-HF)$	94	0.03×10^6	0.05×10^6	70
$(-HCl)$	101	12×10^6	13×10^6	58

[a] These energies are listed with three significant figures only to show that the $CD_3CH_2CH_2OH$ molecules should have slightly more energy than the $CH_3CH_2CH_2OH$ molecules. [b] The calculated rate constant decreases to 2.1×10^5 s^{-1} if the E_0 is increased to 65 kcal mol^{-1}. [c] The numbers in parentheses correspond to adjustment for inefficient collisional deactivtion by SF_6; see text. [d] Taken from ref.[10]

to unit deactivation values. Relaxation of this assumption for $CH_2ClCH_2CH_2OH$ in SF_6 is considered in the Discussion.

The assigned threshold energies are listed in Table 2. The value for dehydration of propanol is 64 kcal mol^{-1}, and the calculated kinetic isotope effect is 2.1 for a common energy of 90 kcal mol^{-1} and $E_0 = 64$ kcal mol^{-1}. If the propanol-d_3 energy is increased to 90.2 kcal mol^{-1}, the calculated isotope effect becomes 2.0. The experimental kinetic-isotope effect was 2.3 $\pm$ 0.2. According to the zero-point energies, the E_0 for propanol and propanol-d_3 are equal. The propanol-d_3 data reinforce the E_0 assignment for dehydration of propanol as 64 kcal mol $^{-1}$. Given the combined uncertainties of the data, the collision cross sections, the approximations in the calculations, and the average nature of E_0 associated with the numerous conformers, the combined uncertainty in E_0 is probably $\pm$2 kcal mol^{-1}.

The threshold energies for $CF_3CH_2CH_2OH$ were assigned as 62 kcal mol^{-1} for elimination of H_2O and 70 kcal mol^{-1} for elimination of HF. For the same $\langle E \rangle$ and E_0, the calculated HF rate constant is 9 times larger than the H_2O elimination rate constant, and that is why E_0(HF) must be $\approx$8 kcal mol^{-1} larger than that for H_2O elimination, even though the experimental rate constants only differ by a factor of 3. A threshold energy of 70 kcal mol^{-1} is typical for HF elimination from the CF_3 group.[12−15]

The experimental rate constant for HCl elimination from $CH_2ClCH_2CH_2OH$ should be reliable, and the assigned threshold energy of 54 kcal mol^{-1} should have a similar uncertainty as for dehydration of propanol; the main caveat is the uncertainty associated with the calculations because of the numerous conformers. The branching fraction for formation of H_2O was only 0.05, and accurate measurement of the small yield of $CH_2ClCH{=}CH_2$ was difficult. The low value selected for the calculated rate constant in Table 2 was a deliberate choice, because we suspect that the experimental rate constant may be too large because the collisional efficiency of SF_6 is questionable. The assigned threshold energy of 59 kcal mol^{-1} for dehydration probably has an uncertainty of $\pm$3 kcal mol^{-1}. The trend for decreasing $E_0(H_2O)$ values in the propanol, trifluoropropanol, chloropropanol series is supported by the DFT calculations.

V. Discussion

The vibrational energy released from recombination of radicals at room temperature have provided a means to study many unimolecular reactions including both rate constants and energy disposal.[2,43] The present study has extended the method to include the CH_2CH_2OH radical, and vibrationally excited $CH_3CH_2CH_2OH$, $CF_3CH_2CH_2OH$, and $CH_2ClCH_2CH_2OH$ molecules were generated, and many other applications using this radical are possible. Although collisional deactivation of highly vibrationally excited alcohols has not been extensively studied, collisions of alkyl iodides with polar alcohol molecules are expected to be as efficient as those with propyl halides,[10,27] and the unit deactivation mechanism employed to obtain the experimental high pressure rate constants should be valid. The only reservation might be for the dual channel reactions with sizable difference in E_0, but lower pressure data would be needed to observe the effects of cascade deactivation[44] on the product branching ratio. The collisional efficiency of SF_6 with vibrationally excited fluoro- and chloroethanes has been studied,[45] and the average energy lost per collision (defined by Lennard-Jones cross sections) was assigned as 5−6 kcal mol^{-1}. For a stepladder model with $\langle \Delta E \rangle = 6$ kcal mol^{-1}, the limiting high pressure rate constant is 1.5 times larger than the unit deactivation result. Modern physical measurements[46,47] of $\langle \Delta E \rangle$ from vibrationally excited molecules such as toluene and pyrazine with colliders similar to SF_6 suggest that the deactivation models are similar or less efficient than the work[45] with the fluoro- and chloroethanes. Therefore we have added a comparison for $CH_2ClCH_2CH_2OH$ with SF_6 bath gas for an experimental rate constant that has been reduced by a factor of 1.5 as an estimate for the unit deactivation result as shown in Table 2. This has the consequence of raising both assigned threshold energies by 1 kcal mol^{-1}.

The 64 kcal mol^{-1} threshold energy assigned to dehydration of propanol is supported by the results from $CD_3CH_2CH_2OH$. Since the thermochemistry for propanol is established and the experimental rate constants seem reliable, the uncertainty in E_0 should be less than $\pm$2 kcal mol^{-1}. The consensus E_0 for ethanol is 66 $\pm$ 2 kcal mol^{-1}. This trend of a small decrease in E_0 with methyl substitution is consistent with the results for propyl chloride and propyl fluoride for which the threshold energies are equal to or slightly (1−2 kcal mol^{-1}) less than the ethyl halides.[10] The comparison in Table 2 shows that $E_0(H_2O)$ is $\sim$5 and $\sim$10 kcal mol^{-1} higher than E_0 for propyl fluoride and propyl chloride, respectively. The lower E_0(HCl) and E_0(HF) explain why thermally activated studies were easier for alkyl chlorides and fluorides than for alcohols. The H_2 elimination

reaction to give propanal has a very high threshold energy and is not competitive with dehydration.

This pattern of higher $E_0(H_2O)$ for alcohols than $E_0(HCl)$ or $E_0(HF)$ for alkyl halides is illustrated by the product branching rates from $CH_2ClCH_2CH_2OH$ for which $E_0(HCl)$ is 5 kcal mol^{-1} lower for HCl elimination and by CH_2FCH_2OH for which E_0 is about 10 kcal mol^{-1} lower for HF elimination.[23] The $E_0(HF)$ from $CF_3CH_2CH_2OH$ does exceed $E_0(H_2O)$ because of the special effect of the CF_3 group for HF elimination.[12] The presence of the CH_2OH group seems not to have seriously affected the E_0 for HCl or HF elimination from $CF_3CH_2CH_2OH$ and $CH_2ClCH_2CH_2OH$. On the other hand the CH_2Cl and CF_3 groups appear to lower the $E_0(H_2O)$ by about 5 and 2 kcal mol^{-1}, respectively. A similar trend for $E_0(H_2O)$ was found by the DFT calculations; the trend is expected to be reliable, even if the actual $E_0(H_2O)$ values are uncertain. Although β-substitution by a F atom tends to raise threshold energies for HX elimination, the effect seems to be rather modest for CH_2FCH_2OH compared to CH_3CH_2OH.[23] The effect of the CF_3 group on $E_0(H_2O)$ mentioned for $CF_3CH_2CH_2OH$ is opposite to that found for HCl and HF elimination reactions;[10,11,13] see Table 2 for an example. Systematic studies are needed to characterize and understand substituent effects on the E_0 values for dehydration reactions of alcohols.

Previous comparisons of transition states for HF and H_2O elimination reactions have noted the similarity of the pre-exponential factors when comparing vibrational models.[2,23] In our case, comparison can be made for propanol and propyl fluoride.[10] The pre-exponential factors (partition function form and $s^\dagger = 1.0$) for C_3H_7F and C_3H_7OH are 3.26×10^{13} and 3.54×10^{13} s^{-1}, respectively, per reaction path at 1000 K for vibrational models. The values are reduced to 0.70×10^{13} and 0.28×10^{13} s^{-1}, respectively, for the hindered-rotor models, and the similarity between the pre-exponential factors for H_2O and HF elimination is diminished. The greater reduction in the pre-exponential factor of propanol arises from the much larger partition function for the OH rotor relative to that for the OH vibrational frequency; the partition functions of the CH_2F and CH_2OH rotors are similar. Although the specific rate constants at 90−100 kcal mol^{-1} are not sensitive to the energy barriers for internal rotation, the partition functions at 1000 K do change with barrier height and the pre-exponential factors can reflect the barrier heights of the rotors. On the basis of the smaller calculated frequency for the CH_3 torsion in the transition state relative to the molecule, we suspect that the rotational barrier may be lower in the transition state than in the propanol molecule and, if so, our pre-exponential factor for propanol may be a lower limit (but only by 20−30% for this particular consideration). If the reaction path degeneracy of 4 is included, the total rate constant for the hindered-rotor model of propanol in Arrhenius form becomes $6.4 \times 10^{13}\ e^{-67.4/RT}$ s^{-1} at 1000 K for $E_0 = 64$ kcal mol^{-1}. This result actually agrees with the report of Maccoll and Thomas.[20]

The pre-exponential factor (partition function form per reaction path) for propyl chloride with a hindered-rotor model[10] is 1.8×10^{13} s^{-1} at 1000 K, and the transition state for HCl elimination has a larger entropy of activation than either HF or H_2O elimination. This also is evident from inspection of the transition-state structures in Figure 5; the C−Cl distance is much longer than the C−O(H) distance.

We also can directly compare the pre-exponential factors for HCl and H_2O elimination from $CH_2ClCH_2CH_2OH$. One important difference is that the HCl transition state has both an OH and a CH_2OH internal rotor, whereas the H_2O transition state has only the CH_2Cl rotor. The pre-exponential factors (partition function form per reaction path) are 2.9×10^{13} and 2.5×10^{13} s^{-1} for HCl and H_2O elimination, respectively, at 1000 K according to vibrational models. These values are reduced to 2.0×10^{13} and 0.23×10^{13} s^{-1} for hindered rotor models, and the consequence of two hindered rotors for the HCl elimination transition state is evident. The calculated OH torsional frequency for the HCl transition state versus the one for HCl elimination was anomalously high. This could be from complex mixing of normal modes and/or a higher barrier to internal rotation than what we have assumed, and the calculated pre-exponential factor for HCl elimination may be overestimated. The similarity of these two pre-exponential factors to those for HCl and H_2O loss from propyl chloride and propanol should be noted. Adding the reaction path degeneracies gives total rate constants in Arrhenius form for $CH_2ClCH_2CH_2OH$ of $13.4 \times 10^{13}\ e^{-56.4/RT}$ and $4.2 \times 10^{13}\ e^{-62.0/RT}$ s^{-1} at 1000 K for E_0 values of 54 and 59 kcal mol^{-1} for HCl and H_2O elimination, respectively.

Since the pre-exponential factor for HF elimination from a CF_3 group has been discussed previously[12] and since the pre-exponential factor for H_2O elimination from $CF_3CH_2CH_2OH$ follows the same pattern as that for $CH_2ClCH_2CH_2OH$, we will just give the total Arrhenius rate constants for HF and H_2O elimination, which are $8.4 \times 10^{13}\ e^{-72.1/RT}$ and $2.3 \times 10^{13}\ e^{-64.2/RT}$ s^{-1}, respectively, at 1000 K for $E_0 = 70$ and 62 kcal mol^{-1}. A common feature for both $CH_2ClCH_2CH_2OH$ and $CF_3CH_2CH_2OH$, the change of the calculated branching ratio for vibrational versus hindered rotational models, is interesting and worth mentioning. This effect was displayed for thermal activation by the ratio of the pre-exponential factors given above for $CH_2ClCH_2CH_2OH$. The same effect also exists for chemical activation rate constants at a single energy. A comparison follows for the sum of states in the transition states of $CH_2ClCH_2CH_2OH$ at 90 kcal mol^{-1} with $E_0 = 60$ kcal mol^{-1}, i.e., 30 kcal mol^{-1} of energy in the transition state. For treatment of the torsional motions as vibrations, the ratio of the sum of states is just 1.02; the ratio increases to 7.5 in favor of HCl elimination for hindered-rotor models. The comparison for $CF_3CH_2CH_2OH$ will be done with 40 kcal mol^{-1} of energy in the transition state since the energy for this system was higher than that for chloropropanol. The ratio of the sums of states for vibrational models is 1.8 in favor of the HF elimination transition state; the ratio increases to 16 for the hindered-rotor model. The larger ratio for the $CF_3CH_2CH_2OH$ system arises because the sum of states for H_2O elimination is nearly the same for treating the CF_3 torsion as a vibration or as an internal rotor with a symmetry number of 3.

A final comparison between the transition states for elimination of HX (X = F, Cl, or OH) is the development of partial charges on individual atoms involved in the four-membered ring. Partial charges on each atom in the molecules and transition states were evaluated using the theory of Atoms In Molecules[48] (AIM) which determines the charges by integrating the electron density (generated at the B3PW91/6-311+G(2d,p) level of theory) for each atom defined by gradient vectors in its electron density. AIM charges are determined by the integration of electron density in the region of a nucleus and, we believe, are therefore better-suited to evaluate partial charges, particularly in situations where there is loose bonding, than the more common Mulliken molecular-orbital based method. An analysis of the partial charges shows that the oxygen atom changes very little between the ground state (−1.1) and the transition state geometry (−1.0). There is a considerable gain of electron density by the carbon atom attached to that oxygen atom (+0.5 in the

ground state, +0.1 in the transition state). The hydrogen atom loses electron density, going from neutral in the ground state to a charge of +0.4 in the transition state geometry, and a slight gain of electron density on the carbon atom formally bonded to that hydrogen atom, from +0.1 to −0.2). There is remarkable similarity between the transition states for HOH and HF loss. The evolution of electron density calculated using AIM for HOH loss is nearly identical, ±0.05, to the AIM charges we calculated for HF loss. In general, the Mulliken charges reported[49] for the HF and HCl elimination transition states are consistent with the AIM electron density that we calculated for similar molecules.

The evolution of electron density for propanol would be consistent with a concerted elimination, rather than an ion-pair type of separation in the transition state. It is tempting to speculate that the mechanism involves elongation of the C−O bond and movement of the proton to one of the lone electron pairs on the oxygen as the electron density in the C−H bond shifts toward the developing double bond between the carbons. The electron density in the C−O bond becomes a lone electron pair of the HOH product. This picture agrees with the cis and trans transition states illustrated by isomers 1 and 2 in Table S-1 in Supporting Information because the proton could transfer to either of the lone pair electrons on the oxygen. There is remarkably little variation (±0.2) in the partial charges of the atoms involved in the HOH elimination transition state geometries across the three alcohols studied here; the replacement of the CH_3 group by a CF_3 or a CH_2Cl group is not affecting the movement of electron density that accompanies the change in geometry from the initial geometry to the transition state geometry.

VI. Conclusions

The photolysis of ICH_2CH_2OH has been used as a source of CH_2CH_2OH radicals at room temperature. Such photolysis in the presence of CH_3I, CD_3I, CH_2ICl, and CF_3I generated chemically activated $CH_3CH_2CH_2OH$, $CD_3CH_2CH_2OH$, and $CH_2ClCH_2CH_2OH$ molecules with 90 kcal mol^{-1} of vibrational energy. Since $D(CF_3-CH_2CH_2OH)$ is larger than $D(CH_3-CH_2CH_2OH)$, the $CF_3CH_2CH_2OH$ molecules have 102 kcal mol^{-1} of vibrational energy. The assignment of the threshold energy for dehydration of propanol was of principal interest, and 64 ± 2 kcal mol^{-1} was established as the $E_0(H_2O)$ for loss of H_2O from propanol by comparing the experimental rate constant to calculated statistical (RRKM) rate constants that were based on models from electronic structure calculations. The torsional motions in the molecules and transition states were treated as hindered internal rotations in the calculations. The competition between dehydration (or elimination of H_2O) and HCl or HF elimination from $CH_2ClCH_2CH_2OH$ and $CF_3CH_2CH_2OH$ was analyzed. The transition state for elimination of H_2O has a somewhat smaller entropy of activation than that for elimination of HF or HCl. The chemical activation technique permits the study of the unimolecular dehydration reaction without the complications arising from the free-radical reactions that affect thermal activation studies of alcohols.

A recent computational study[50] of the unimolecular decomposition pathways in propene-2-ol predicts that H migration by a four-centered transition state giving acetone has the lowest threshold energy barrier (54 kcal). Subsequently, acetone decomposes by loss of a methyl radical. The 1,2- and 2,3-HOH elimination channels have high threshold energies, 80−81 kcal mol^{-1}, because of substituent or structural effects in the transition states. The 1,2-HOH elimination to form an alkyne is probably characteristic for an OH located adjacent to a double bond. This investigation of propene-2-ol and our finding that CF_3 and CH_2Cl groups seem to reduce the threshold energy for dehydration relative to that for propanol suggest that additional studies of these substituent effects is warranted. The importance of treating torsional motions as appropriate hindered internal rotations should be remembered.[51]

Acknowledgment. Financial support for this work was provided by the US National Science Foundation under Grant CHE-0647582. Brooke Siblia and Jacqueline Quintrall are thanked for assistance with data collection.

Supporting Information Available: Tables S-1 ($CH_3CH_2CH_2OH$), S-2 ($CF_3CH_2CH_2OH$), and S-3 ($CH_2ClCH_2CH_2OH$) list the calculated vibrational frequencies, overall moments of inertia, and the reduced moments of inertia for the internal rotors, the same information is listed for the transition state for loss of HCl, HF, or HOH, the relative energies for each conformer of the reactant are shown relative to the lowest energy conformer and the computed threshold energies are listed for the transition states, the geometric means that were used in the calculation of the unimolecular rate constants are listed, and the computed structure for each conformer of the reactant and of the transition state is also shown. This information is available free of charge via the Internet at http://pubs.acs.org.

References and Notes

(1) (a) Goodale, J. W.; Evans, D. K.; Ivanco, M.; McAlpine, R. D. *Can. J. Chem.* **1990**, *68*, 1437. (b) Holbrook, K. A.; Oldershaw, G. A.; Shaw, C. J. *Int. J. Chem. Kinet.* **1993**, *25*, 323. (c) Danen, W. C. *J. Am. Chem. Soc.* **1979**, *101*, 1187.

(2) (a) Butkovskaya, N. I.; Zhao, Y.; Setser, D. W. *J. Phys. Chem.* **1994**, *98*, 10779. (b) Butkovskaya, N. I.; Setser, D. W. *J. Phys. Chem.* **1996**, *105*, 8004. (c) Butkovskaya, N. I.; Setser, D. W. *Int. Rev. Phys. Chem.* **2003**, *22*, 1.

(3) (a) Li, J.; Kazakov, A.; Dryer, F. L. *J. Phys. Chem. A* **2004**, *108*, 7671. (b) Li, J.; Kazakov, A.; Dryer, F. L. *Int. J. Chem. Kinet.* **2001**, *33*, 859.

(4) Tsang, W. *Int. J. Chem. Kinet.* **2004**, *36*, 456.

(5) Park, J.; Zhu, R. S.; Lin, M. C. *J. Chem. Phys.* **2002**, *117*, 3224.

(6) Tsang, W. *Int. J. Chem. Kinet.* **1976**, *8*, 193.

(7) Park, C. R.; Wisenfeld, J. R. *J. Chem. Phys.* **1991**, *95*, 8166.

(8) (a) Shu, J.; Lin, J. J.; Lee, Y. T.; Yang, X. *J. Chem. Phys.* **2001**, *115*, 849. (b) Kohguchi, H.; Ogi, Y.; Suzuki, T. *Phys. Chem. Chem. Phys.* **2008**, *10*, 7222.

(9) Dorer, F. H.; Rabinovitch, B. S. *J. Phys. Chem.* **1965**, *69*, 1973.

(10) (a) Ferguson, J. D.; Johnson, N. L.; Keknes-Husker, P. M.; Everett, W. C.; Heard, G. L.; Setser, D. W.; Holmes, B. E. *J. Phys. Chem. A* **2005**, *109*, 4540. (b) Zhu, L.; Simmons, J. G., Jr.; Burgin, M. O.; Setser, D. W.; Holmes, B. E. *J. Phys. Chem. A* **2006**, *110*, 1506.

(11) Booze, J. A.; Baer, T. *J. Phys. Chem.* **1992**, *96*, 5715.

(12) Holmes, D. A.; Holmes, B. E. *J. Phys. Chem. A* **2005**, *109*, 10726.

(13) (a) Burgin, M. O.; Simmons, J. G., Jr.; Heard, G. L.; Setser, D. W.; Holmes, B. E. *J. Phys. Chem. A* **2007**, *111*, 2283. (b) Beaver, M. R.; Simmons, J. G., Jr.; Heard, G. L.; Setser, D. W.; Holmes, B. E. *J. Phys. Chem. A* **2007**, *111*, 8445.

(14) (a) Zaluzhna, O.; Simmons, J. G., Jr.; Heard, G. L.; Setser, D. W.; Holmes, B. E. *J. Phys. Chem. A* **2008**, *112*, 6090. (b) Zaluzhna, O.; Simmons, J. G., Jr.; Setser, D. W.; Holmes, B. E. *J. Phys. Chem. A* **2008**, *112*, 12117.

(15) Lisowski, C. E.; Duncan, J. R.; Heard, G. L.; Setser, D. W.; Holmes, B. E. *J. Phys. Chem. A* **2007**, *111*, 8445.

(16) Kalra, B. L.; Lewis, D. K.; Singer, S. R.; Raghavan, A. S.; Baldwin, J. E.; Hess, B. A., Jr. *J. Phys. Chem. A* **2004**, *108*, 11554.

(17) Bishop, M.; Holbrook, K. A.; Oldershaw, G. A.; Dyer, P. E. *Int. J. Chem. Kinet.* **1994**, *26*, 201.

(18) Trenwith, A. B. *J. Chem. Soc., Faraday Trans. 1* **1975**, *71*, 2405.

(19) Barnard, J. A.; Hughes, H. W. D. *Trans. Faraday Soc.* **1960**, *56*, 64.

(20) Maccoll, A.; Thomas, P. J. *Prog. React. Kinet.* **1967**, *4*, 119.

(21) Bui, B. H.; Zhu, R. S.; Lin, M. C. *J. Chem. Phys.* **2002**, *24*, 11188.

(22) Shu, J.; Lin, J. J.; Lee, Y. T.; Yang, X. *J. Am. Chem. Soc.* **2001**, *123*, 322.

(23) Rajakumar, B.; Reddy, K. P.; Arunan, E. *J. Phys. Chem. A* **2003**, *107*, 9782.
(24) Anastasi, C.; Simpson, V.; Munk, J.; Pagsberg, P. *J. Phys. Chem.* **1990**, *94*, 63227.
(25) Jenkins, M. E.; Cox, R. A. *J. Phys. Chem.* **1991**, *95*, 3229.
(26) Holmes, J. L.; Lossing, F. P. *J. Am. Chem. Soc.* **1986**, *108*, 1086. 1982, *104*, 2648.
(27) McDowell, D. R.; Weston, J.; Holmes, B. E. *Int. J. Chem. Kinet.* **1996**, *28*, 61.
(28) (a) Sapers, S. P.; Hess, W. P. *J. Phys. Chem.* **1992**, *97*, 3126. (b) Hintsa, E. J.; Xinsheng, Z.; Lee, Y. T. *J. Chem. Phys.* **1990**, *92*, 2280.
(29) Holmes, B. E.; Paisley, S. D.; Rakestraw, D. J.; King, E. E. *Int. J. Chem. Kinet.* **1986**, *18*, 639.
(30) Mourtis, F. M.; Rummeurs, F. H. A. *Can. J. Chem.* **1977**, *55*, 3007.
(31) Hipper, H.; Troe, J.; Wendelken, H. J. *J. Chem. Phys.* **1983**, *78*, 6709.
(32) Berkowitz, J.; Ellison, G. B.; Gutman, D. *J. Phys. Chem.* **1994**, *98*, 2244.
(33) Fulle, D.; Hamann, H. F.; Hippler, H.; Jänsch, C. P. *Ber. Bunsen-Ges. Phys. Chem.* **1997**, *101*, 1433.
(34) Kerr, J. A.; Stocker, D. W. Standard Thermodynamic Properties of Chemical Substances. In *Handbook of Chemistry and Physics*; Linde, D. R., Jr., Ed.; CRC Press: Boca Raton, FL, 2007.
(35) Zachariah, M. R.; Westmoreland, P. R.; Burgess, D. R., Jr.; Tsang, W.; Melius, C. F. *J. Phys. Chem.* **1996**, *100*, 8737.
(36) Khursan, S. L. *Russ. J. Chem. Phys. (Engl. Transl.)* **2004**, *78* (1), S34.
(37) Barker, J. R. *Int. J Chem. Kinet.* **2001**, *33*, 232.
(38) Frisch, M. J.; Trucks, G. W.; Schlegel, H. B.; Scuseria, G. E.; Robb, M. A.; Cheeseman, J. R.; Montgomery, J. A., Jr.; Vreven, T.; Kuden, K. N.; Burant, J. C.; Millam, J. M.; Iyengar, S. S.; Tomasi, J.; Barone, V.; Mennucci, B.; Cossi, M.; Scalmani, G.; Bega, N.; Petersson, G. A.; Nakatsuji, H.; Hada, M.; Ehara, M.; Toyota, K.; Fukuda, R.; Hasegawa, J.; Ishida, M.; Nakajima, T.; Honda, Y.; Kitao, O.; Adamo, C.; Jaramillo, J.; Gomperts, R.; Stratman, R. E.; Yazyev, O.; Austen, A. J.; Cammi, R.; Pomelli, C.; Ochterski, J. W.; Ayala, P. Y.; Morokuma, K.; Voth, G. A.; Salvador, P.; Dannenberg, J. J.; Zakrzewksi, V. G.; Dapprich, S.; Daniels, A. D.; Strain, M. C.; Farkas, O.; Malik, D. K.; Rabuck, A. D.; Raghavachari, K.; Foresman, J. B.; Ortiz, J. V.; Cui, Q.; Baboul, A. G.; Clifford, S.; Cioslowski, J.; Stefanov, B. B.; Liu, G.; Liashenko, A.; Piskorz, P.; Komaromi, I.; Martin, R. L.; Fox, D. J.; Keith, T. Al-Laham, M. A.; Peng, C. Y.; Nanayakkara, A.; Challacombe, M.; Gill, P. M. W.; Johnson, B.; Chen, W.; Wong, M. W.; Gonzalez, C. Pople, J. A. *Gaussian 03, Revision B.04*; Gaussian, Inc.: Pittsburgh, PA, 2003.
(39) Lotta, T.; Murto, J.; Räsänen, M.; Aspiala, A. *Chem. Phys.* **1984**, *86*, 105.
(40) Takahashi, K.; Sugawara, M.; Yabushita, S. *J. Phys. Chem. A* **2003**, *107*, 11092.
(41) Jarmelo, S.; Maiti, N.; Anderson, V.; Carey, P. R.; Fausto, R. *J. Phys. Chem. A* **2005**, *109*, 2069.
(42) Yamanaka, T.; Kawasaki, M.; Hurley, M. D.; Wallington, T. J.; Xian, L.; Schneider, W. F. *J. Phys. Chem. A* **2008**, *112*, 2773.
(43) (a) Lipeng, S.; Park, K.; Song, K.; Setser, D. W.; Hase, W. L. *J. Chem. Phys.* **2006**, *124*, 64313. (b) Dong, E.; Setser, D. W.; Hase, W. L.; Song, K. *J. Phys. Chem. A* **2006**, *110*, 1484. (c) Setser, D. W.; Muravyov, A. A.; Rengarajan, R. *J. Phys. Chem. A* **2004**, *108*, 3745.
(44) Holbrook, K. A.; Pilling, M. J.; Robertson, S. H. *Unimolecular Reactions*, 2nd ed.; John Wiley and Sons: New York, 1996.
(45) (a) Richmond, G.; Setser, D. W. *J. Phys. Chem.* **1980**, *84*, 2699. (b) Marcoux, P. J.; Setser, D. W. *J. Phys. Chem.* **1978**, *82*, 97.
(46) (a) Du, J.; Yuan, L.; Shizuka, H.; Lin, F.; Mulin, A. S. *J. Phys. Chem. A* **2008**, *112*, 9396. (b) Liu, Q.; Havey, D. K.; Mullin, A. S. *J. Phys. Chem. A* **2008**, *112*, 9509. (c) Miller, L. A.; Barker, J. A. *J. Chem. Phys.* **1996**, *105*, 1383.
(47) (a) Lenzer, T.; Luther, K.; Reihs, K.; Symonds, A. C. *J. Chem. Phys.* **2000**, *112*, 4090. (b) Hold, U.; Lenzer, T.; Luther, K.; Symonds, A. C. *J. Chem. Phys.* **2003**, *119*, 11192.
(48) Bader, R. F. W. *Atoms In Molecules, A Quantum Theory*; Clarendon Press: Oxford, 1990.
(49) Toto, J. L.; Pritchard, G. O.; Kirkman, B. *J. Phys. Chem.* **1994**, *98*, 8359.
(50) Zhou, L. *J. Chem. Phys.* **2008**, *129*, 234301.
(51) Weiz, O.; Striebel, F.; Olzmann, M. *Phys. Chem. Chem. Phys.* **2008**, *10*, 320.

JP905012R